

# The Design and Evaluation of Three-dimensional Corner Joints Used in Wooden Furniture Frames: Experimental and Numerical

Bingrui Chen,<sup>a,b</sup> Haiyan Xia,<sup>a</sup> and Wengang Hu<sup>a,b,\*</sup>

This study aimed to design and evaluate the detachable corner joints used in wooden furniture frames, including a commonly used detachable joint (control) form using mortise and tenon with plug reinforcement and three novel proposed joints, *i.e.*, novel joint I ~ III, which adopted in-line double-hole nuts, metal sheet connector, and embedded nuts and screws respectively, *via* numerical and experimental methods. The numerical analysis results indicated that the optimal proposed joint (novel joint I) had good mechanical performance when subjected to bending load with proper stress distributions and relatively low maximum stress compared with the other two proposed joints. The experimental results showed that the bending load resistance of the control and the optimal proposed joints were 1920 N (0.14) and 4390 N (0.05), respectively. The bending moment capacity and bending stiffness of the optimal joints were remarkably higher than the bending moment capacity and bending stiffness of the control joint. In addition, the combination of the numerical and experimental methods could effectively simplify the steps of furniture connection design and development and save costs in terms of time and materials.

DOI: 10.15376/biores.17.2.2143-2156

Keywords: Wood furniture frames; Corner joint; Bending moment capacity; Finite element method

Contact information: a: Department of Furniture Design, College of Furnishings and Industrial Design, Nanjing Forestry University, Nanjing 210037 China; b: Co-Innovation Center of Efficient Processing and Utilization of Forest Resources, Nanjing Forestry University, Nanjing 210037 China;  
\* Corresponding author: hwg@njfu.edu.cn

## INTRODUCTION

Wood furniture joints constitute the critical but sensitive elements of furniture construction, which often resist the internal and external forces imposed upon them during service (Eckelman 1978). Therefore, the design of the joints in a wooden furniture frame is far more important than the entire design process (Eckelman 2003). It is more likely caused by joint failure or damage rather than the breakage or fracture of its members when the wooden furniture frame, *i.e.*, the side frame of chairs, fail during service (Eckelman 2003; Eckelman and Haviarova 2006). Traditional mortise-and-tenon (M&T) joints are widely used in wooden furniture frames (Erdil *et al.* 2005; Wu *et al.* 2020). Previous investigations conducted found several critical factors influencing the service life of M&T joints, *e.g.*, moisture, wood species, adhesive type, heat treatment, tenon size, and tenon geometry (Likos *et al.* 2012; Hajdarevic and Martinovic 2014; Zhou *et al.* 2018; Yan *et al.* 2020; Liu *et al.* 2019; Yang and Liu 2020; Zhou *et al.* 2020; Fu *et al.* 2021a; Yin and Liu 2021; Wu *et al.* 2021).

Despite the gradual rise of online sales and ready-to-assemble (RTA) furniture, the detachable connection type has become the mainstream of furniture structural design. Case furniture already has relatively mature connectors, *e.g.*, the most popular eccentric joint. However, due to the effects of adhesive, glued wooden M&T joints, which are widely used in wood furniture frames, have always been regarded as a permanent joint (Ratnasingam and Ioras 2013; Zhao *et al.* 2020). Furthermore, the glued M&T joints are labor-intensive and have higher costs in terms of machining compared with detachable joints. In addition, they are quite difficult to repair; once the joint is loose or damaged, it results in the scrapping of the whole furniture product (Uysal *et al.* 2015). For these reasons, novel connectors have been designed and proposed as furniture joints. Podskarbi *et al.* (2017) summarized the technical rules for designing new connections for furniture joints: They should be easy to assemble and disassemble, have a minimum number of components, meet aesthetic requirements, and be externally invisible. Krzyżaniak *et al.* (2020) designed novel connections by using 3D printing technology for RTA furniture and analyzed the effects of internal mounting forces and selected materials on the stiffness and bending moment capacity (BMC) of the joints.

With the rapid development of computer technology, previous studies have confirmed that numerical simulation, *e.g.*, the finite element method (FEM), is an effective method commonly used to simulate the mechanical properties and behavior of wood-based structures (Li *et al.* 2020; Fu *et al.* 2021b). In recent years, the M&T joints used in wood furniture were simulated using the FEM to evaluate and predict the static and fatigue strength (Kasal *et al.* 2016; Chen and Wu 2018; Xi *et al.* 2020; Yu *et al.* 2021). Under the premise of establishing a reasonable joint model, FEM has been proven to have a relatively high accuracy and allows for the visualization of the stress distribution. Hu and Liu (2020) compared three types of M&T joint finite element models, which confirmed that the semi-rigid model performed better to simulate the bending strength of wood joints. Zor and Kartal (2020) further verified the validity of using a semi-rigid joint model in simulating furniture corner joints *via* FEM. Kaygin *et al.* (2016) tested the diagonal compression and tension of corner joints based on simulation and experimental methods, which were carried out using dowel and M&T elements. The results showed that the amount of deformation obtained from the experiments was consistent with the FEM computer modeling *via* ANSYS with 90% to 97% agreement, which implies that it can be used in furniture design and engineering. Krzyżaniak and Smardzewski (2021) designed and tested a novel fastener under dynamic loading conditions. However, the previous studies primarily focused on providing an effective way to evaluate the strength properties of traditional connecting methods; few researchers tried to obtain the optimal design of a joint *via* FEM.

The primary objective of this study was to design and evaluate the detachable corner joints used in wooden furniture frames, which have the advantages of easy manufacturing and disassembling.

In order to realize the objective, numerical and experimental methods were used to investigate the stress distributions and magnitudes of a commonly used detachable joint (control) and three novel proposed joints when subjected to bending strength. This study will contribute to reducing the costs of furniture connection design and development by using numerical analysis and experimental methods.

## EXPERIMENTAL

### Materials

The experimental material was beech (*Fagus orientalis*), which was bought from a local lumber merchant (Nanjing, China). The specific gravity averaged 0.65 g/cm<sup>3</sup>, according to ASTM standard D2395 (2010). The moisture content (MC) was conditioned to and held at 8.80% to 9.46% before and during the experiment tested according to ASTM standard D4442 (2010). In addition, all hardware connectors were made of low-carbon steel and were also bought from the local commercial shop (Nanjing, China).

Table 1 shows the basic mechanical properties of beech wood, which were tested in a previous study by the authors (Hu *et al.* 2021), and low-carbon steel. All these mechanical properties were assigned to the proposed finite element model.

**Table 1.** Mechanical Properties of Beech Wood and Low-carbon Steel (Unit: mm)

Materials	Elastic Modulus (MPa)			Poisson's Ratio			Shear Modulus (MPa)			Yield Strength (MPa)
	$E_L$	$E_R$	$E_T$	$\nu_{LR}$	$\nu_{LT}$	$\nu_{RT}$	$G_{LR}$	$G_{LT}$	$G_{RT}$	
Beech wood	12205	1858	774	0.502	0.705	0.526	899	595	195	53.62
Steel	210000			0.28			/			620.44

Note:  $E$  is elastic modulus (MPa);  $\nu$  is Poisson's ratio;  $G$  is shear modulus (MPa); L, R, and T refer to the longitudinal, radial, and tangential directions of beech wood, respectively.

### Experimental Design

This study was divided into three stages: 1) three newly proposed corner joints composed of two rails and a post leg were designed; 2) with the aim of obtaining the optimal joint out of the three novel designs, the finite element models were established to evaluate the three novel proposed corner joints and one commonly used detachable joint (control) according to bending load performance; and 3) experimental tests were conducted to compare the control joint with the optimal joint when subjected to the bending moment capacity (BMC) and bending stiffness with 10 replications for each.

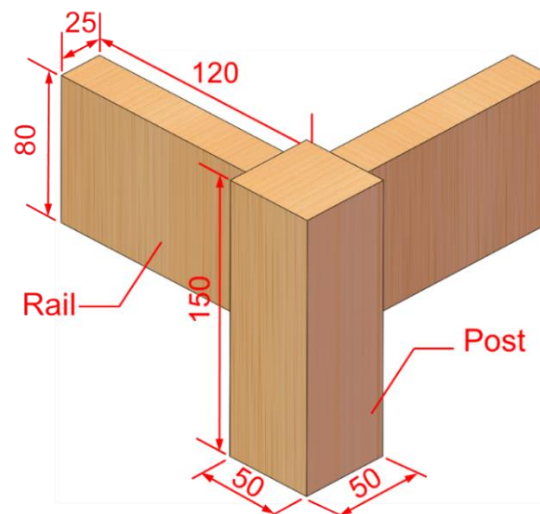


**Fig. 1.** Dimensions of the corner joints used in wooden furniture frames (Unit: mm)

## Design of the Joints and Specimen Preparation

### *Configurations of the specimen*

The design of each corner joint and its corresponding members were the same sizes, as shown in Fig. 1. Each joint consisted of two rails, which measured 25 mm by 80 mm in the cross-section by 150 mm long, while the post leg measured 50 mm square by 150 mm.

### *Commonly used detachable joint*

The commonly used detachable joint form using mortise and tenon (M&T) with plug reinforcement is shown in Fig. 2. This type of joint has been widely used in furniture frames according to the previous investigation (Chen and Xu 2017). The post and rails were connected with the M&T constructed with a computer-numerical-control based (CNC) machine (WPC, ULI, Shanghai, China) with an accuracy of 0.01 mm. The mortise was drilled in the post member, and the tenon was machined in the cross-section of the post members. The dimensions of the mortise (and matching tenon) measured 15 mm (length)  $\times$  10 mm (height)  $\times$  40 mm (width). The joints were reinforced with 20 mm long by diameter 8 mm bolts to connect the metal plug corner with the post leg. In addition, three screws, which measured 16 mm long with a diameter of 4 mm, were passed through the metal plug and connected with the rail. The end of the metal plug was bent into the slot of the side rail, which measured 60 mm in length and 7 mm in depth.

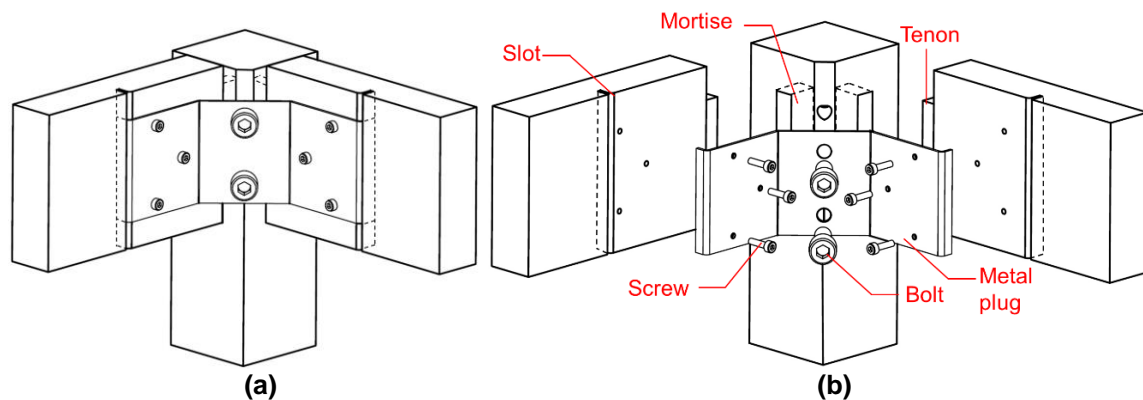


**Fig. 2.** Schematic diagram of the commonly used detachable joint: (a) assembly view; and (b) explosive view

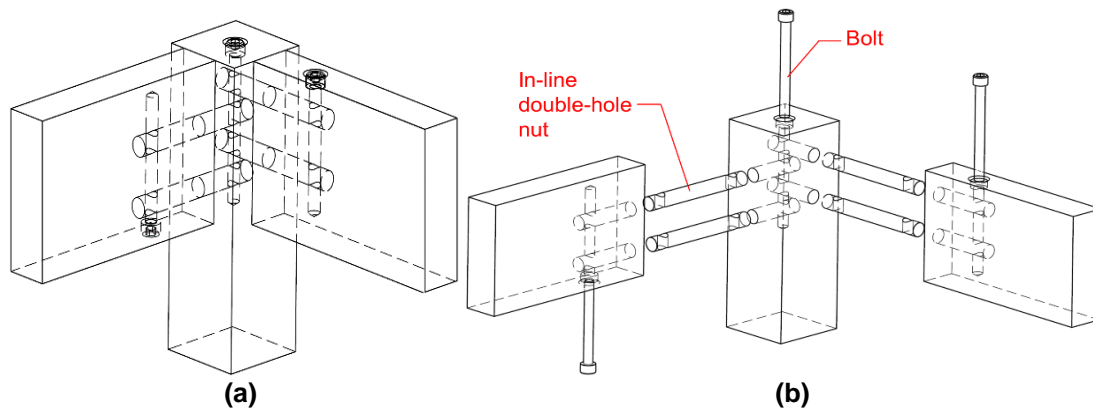


**Fig. 3.** Schematic diagram of the novel joint I: (a) assembly view; and (b) explosive view

### Novel joint I

The novel joint I adopted four in-line double-hole nuts to connect and provided strength between the post and rails instead of using M&T for manufacturing and assembling (as shown in Fig. 3). The nuts, which measured 84 mm long with a diameter of 6 mm, were inserted into the relief holes drilled on the post leg and rails. The nuts were fastened with 50 mm and 60 mm long bolts, both with a diameter of 6 mm, which passed through and fixed the rail members and post legs, respectively.

### Novel joint II

The novel joint II was constructed with a sheet metal connector to concatenate two rails and reinforce the joint, as shown in Fig. 4. The metal sheet connector, which was in the shape of the letter “W”, had one side inserted into the slotted hole in the rail, with a length of 80 mm, while the bent part of the sheet, with a length of 30 mm, was attached to the open hole of the post, which was drilled by the CNC. The metal sheet connector measured 31.5 mm wide by 3 mm thick. Self-tapping screws, with a diameter of 6 mm that were 14 mm long, were chosen to fasten the sheet connector and wood members.

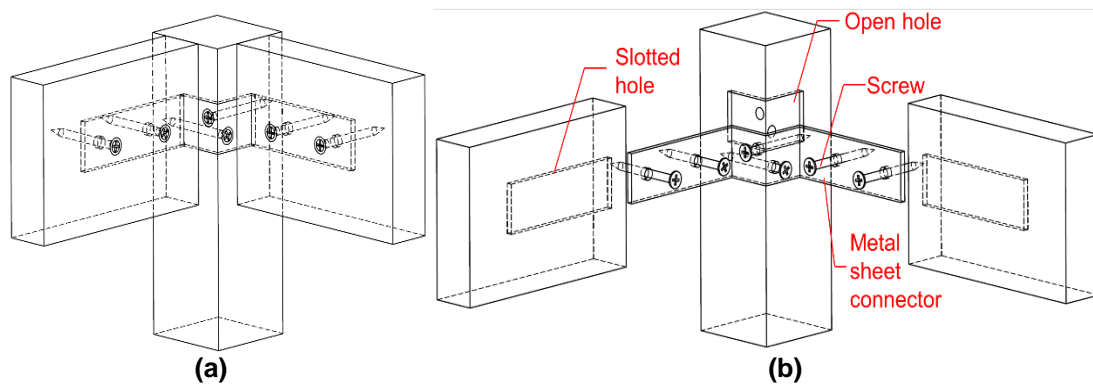


Fig. 4. Schematic diagram of the novel joint II: (a) assembly view; and (b) explosive view

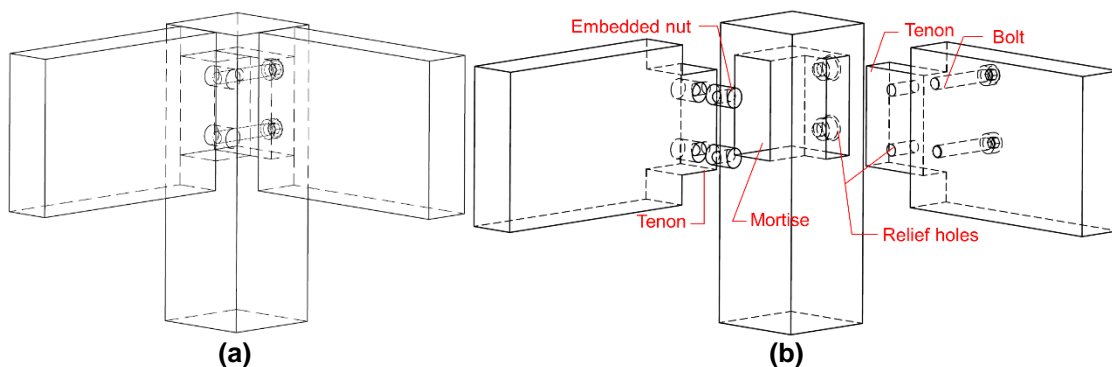


Fig. 5. Schematic diagram of the novel joint III: (a) explosive view; and (b) assembly view

### Novel joint III

Compared with the control joint, the novel joint III, replaced the exposed metal plug and bolt by using embedded nuts and screws to reinforce the rectangular M&T components. As shown in Fig. 5, two nuts with a diameter of 8 mm were embedded in the tenon of one rail member, while another rail member and the side wall of the post leg were

provided with two relief holes for the bolts to pass through. During assembly, the bolts sequentially passed through the wood members and finally engaged with the nuts. This structure has obvious advantages in terms of the invisibility of the hardware connectors, which users can easily purchase and assemble with several simple steps.

### Numerical Simulation Method

The finite element models of the four corner joints were established according to the configurations shown in Figs. 2 through 5 using commercial modeling software (SolidWorks 2017, Dassult Systèmes, Vélizy-Villacoublay, France). The mechanical properties used in this model were assigned from the beech and low-carbon steel values shown in Table 1; the yield strength was taken as a stress criterion. With the aim of reducing the computing time, the finite element models were simplified by removing unnecessary decoration and stress-free fillet. All components and connectors were assembled in the software, while the toolbox in SolidWorks was used as the fasteners. All freedoms of the bottom of the post leg were constrained, and a 1000 N load was applied at the point 90 mm from the end of rail member. The interactions between the post, rail members and the fasteners were set to the non-penetrating contact mode in the software. The loading conditions used are shown in Fig. 6a, and the BMC and bending stiffness were considered as critical criteria to evaluate the strength of furniture joints. The mesh of the model in SolidWorks Simulations is shown in Fig. 6b, which was chosen by the Voronoi-Delaunay mesh scheme. The maximum element size was 0.50 mm, and the minimum element size was 9.96 mm.

In this study, the stress distributions of the finite element models of the four corner joints, which consisted of a control joint and three novel joints, were compared when subjected to the bending strength through the numerical simulation method. Furthermore, the output stress distributions, maximum stress magnitudes, machining difficulty, and other indexes were taken into consideration. After the comparison, the control joint and the optimal novel joint would be selected for further study.

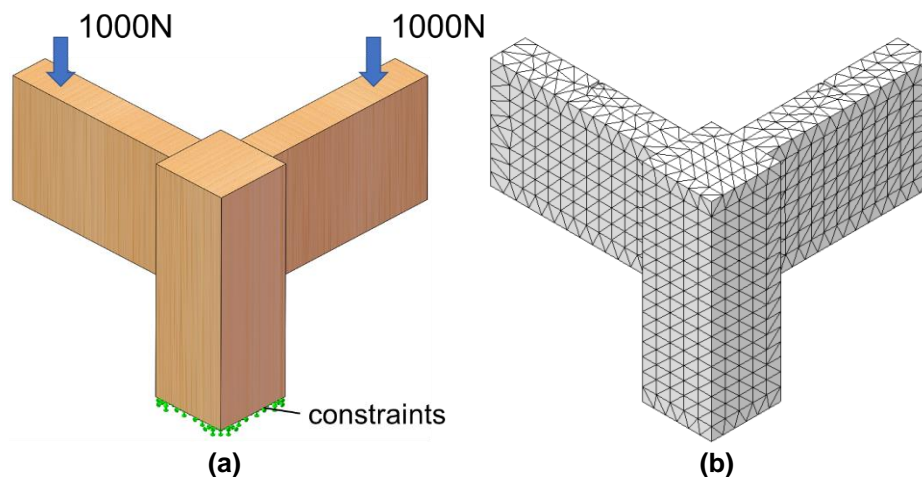


**Fig. 6.** The finite element model used to simulate the stress distributions and maximum stress magnitudes of four corner joints: the load and constraints condition (a); and meshed model (b)

## Testing Method

In order to quantify the strength of the improved corner joints and verify the effectiveness of the finite element model, experiments were carried out to measure the BMC and stiffness of the control joints and novel joint I, which performed better in the numerical simulation; the testing set up is shown in Fig. 7. The equipment used in this experiment was a universal testing machine (AG-X, 20kN, Shimadzu, Japan). First, the post leg was constrained with the metal fixtures, while the load was imposed on one side of the rail, with the loading position 90 mm from the edge of the post by the loading head, at a speed of 5 mm/min, until the displacement reached 50 mm. Second, the rail on the other side of the test specimen was used as a replication sample, and the loading position and speed were consistent. In addition, ten corner joints of the control and novel joint I were constructed in the same way, and for replication purposes the specimens were tested to determine the BMC and bending stiffness.

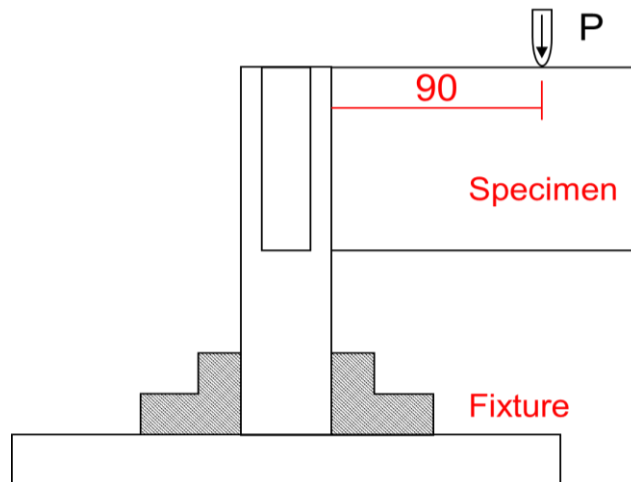


Fig. 7. Setup for measuring the bending moment load of the selected corner joints (Unit: mm)

Testing joints with the bending loads and deflections were obtained in the experimental method described above. The BMC and bending stiffness values were calculated according to Eqs. 1 and 2, respectively,

$$M = F \times L \quad (1)$$

$$K = \Delta F / \Delta d \quad (2)$$

where  $M$  is the bending moment capacity (N·m),  $P$  is the bending load (N),  $L$  is the moment arm (mm),  $K$  is the bending stiffness (N/mm),  $\Delta F$  is the change force in the linear portion of bending load and deflection curve (mm), and  $\Delta d$  is the change of deflection corresponding to  $\Delta F$  (mm).

## RESULTS AND DISCUSSION

### Results of Numerical Simulations

Figure 8 shows the stress distributions and magnitudes of the four corner joints, which were output from the SolidWorks simulation.

Figure 8a shows the stress distribution of the commonly used detachable joint (control); the maximum stress was 245.2 MPa, which was at the bent part of the metal plug. Furthermore, the maximum stress of the wood component appears at the edge of the relief hole through which the screw passes.

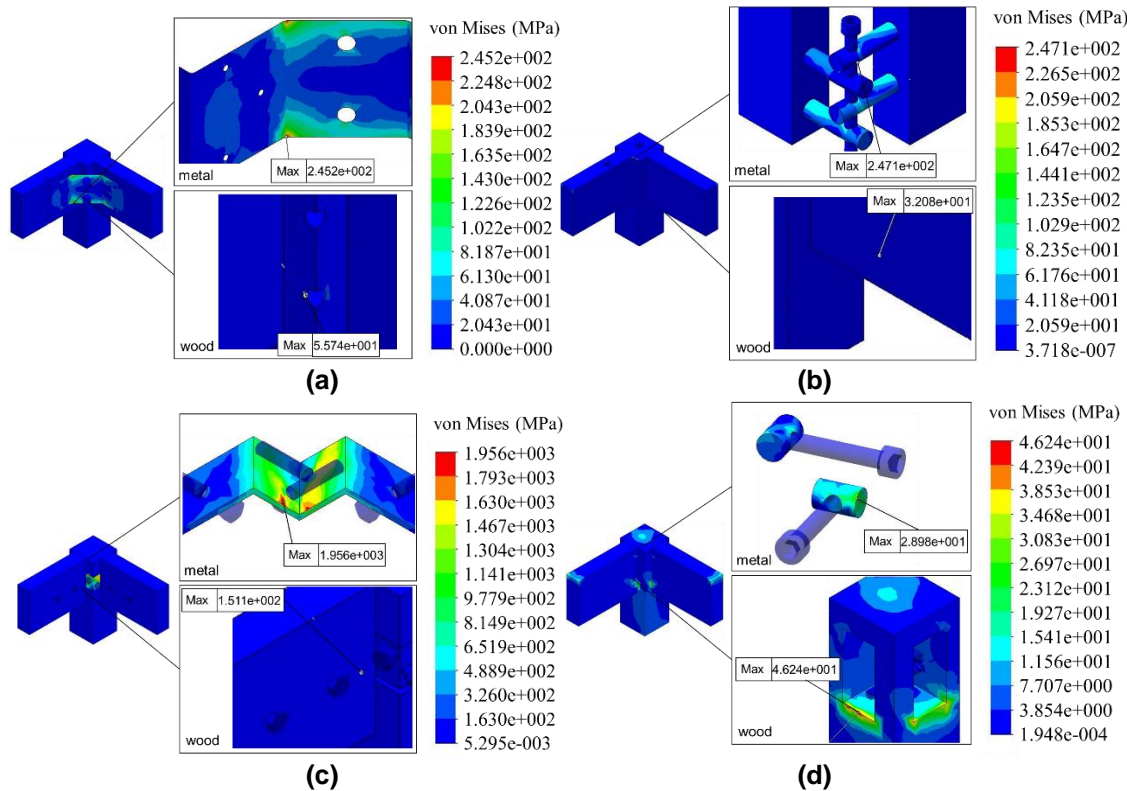


**Fig. 8.** Stress distributions of the corner joint: commonly used detachable joint (a); novel joint I (b); novel joint II (c); and novel joint III (d)

Figure 8b shows the stress distribution of novel joint I; the maximum stress was 247 MPa, which was concentrated at the intersection of the nuts and bolts inside the post member. Compared with the control joint, the stresses of the wood members were much less than the stress of the control joint, which concentrated on the side of rail member. While the stress of the metal connectors increased slightly, approximately 1.7 MPa, due to the connection type. Generally, the stress concentration was still far less than the yield strength of the material itself. In addition, this joint has the obvious advantages of easy processing and disassembly. Users can easily take down and replace the wood components or metal connectors with simple tools in case the furniture frame is damaged.

Figure 8c shows the stress distribution of novel joint II; the maximum stress appears at the metal connector sheet (245.7 MPa), which is due to the stress concentration caused by the bending of the end distance, while the maximum stress of the wood was 151.1 MPa, which was located at the edge of the open hole. The stress concentrate on the wood rail and metal connector far exceeded the yield strength of the material itself, which meant that it will soon fail in this loading mode. This result may be caused by excessive bending of the sheet metal connectors. At the same time, the connection between the metal and wood components will loosen due to the existence of slotted holes, which will lead to the decline of the joint strength.

The last joint, novel joint III, is shown in Fig. 8d, with a maximum stress of 46.24 MPa, which was concentrated on the edge of the mortise on the post member, while the metal connections stress was 28.98 MPa, which was less than the wood component. The primary reason for this was that the tenon and mortise bore an additional portion of the load, while the embedded nut and screw primarily played a stabilizing role in this case. Therefore, this connection type will not be recommended for furniture joints made of fast-growing wood.

According to the numerical simulation results, the stress distributions of the wood members and metal connections were analyzed. Obviously, the optimal proposed joint was novel joint I, which showed better performance with a lower stress concentration on the post and rail leg members as well as being easy to manufacture and disassemble. Further study will be based on these two connecting types through the experimental method.

## Experimental Results

### *Bending moment capacity (BMC) and bending stiffness of the experimental joints*

The results of the average bending load-deflection are graphically illustrated in Fig. 9. The maximum average bending load of the control joint and the optimal proposed joint (novel joint I) were 1920 N (0.14) and 4390 N (0.05), respectively. Compared with the control joint, the bending strength of the novel joint I had remarkably increased by over 200%, which was primarily due to the proper stress distributions and relatively lower maximum stress of the wood members. In addition, the coefficient of variation (COV) of the two tested joints conveyed that the optimal novel joint was more stable than the control joint in terms of bending resistant strength.

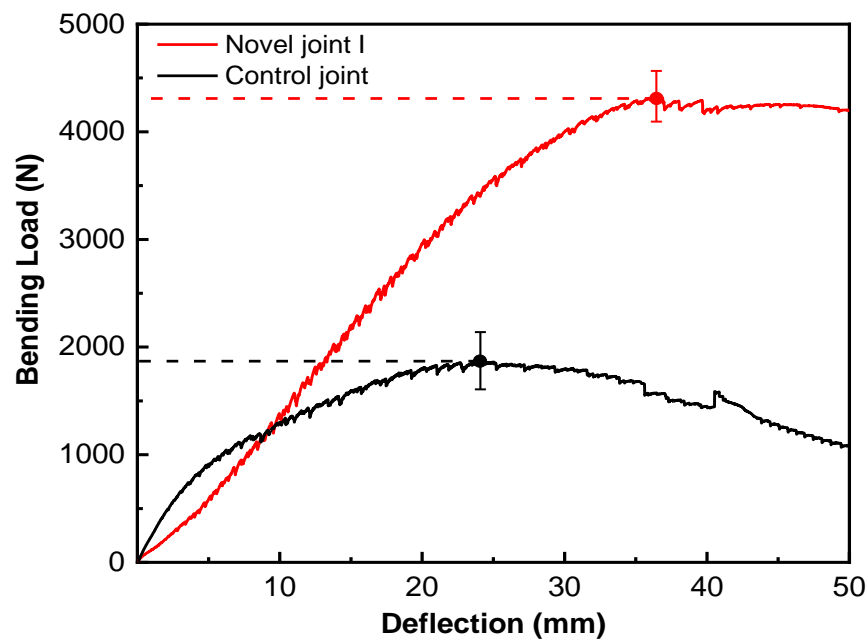


**Fig. 9.** The deflection-bending load curves of the two tested joints

The results of the average BMC and bending stiffness of the corner joints with different connection types with their COV are given in Table 2. As shown in Table 2, both the BMC and bending stiffness of novel joint I were much higher than the BMC and

bending stiffness of the control joint. The BMC of the optimal joint increased approximately two-fold, and the bending stiffness increased by 153%.

**Table 2.** Mean Bending Moment Capacity and Stiffness of Corner Joints with Different Connect Types

Connector Types	Bending Moment Capacity (N·mm)	Bending Stiffness (N/mm)
Control	173 (0.14)	73.6
Novel joint I	395 (0.05)	113

Note: the values in parentheses are coefficients of variation.

#### *Failure mode analysis*

In general, both the control joint and the novel joint I failed completely under the deflection of 50 mm. Figure 10 summarizes the typical failure modes of all tested specimens with two different connecting types.

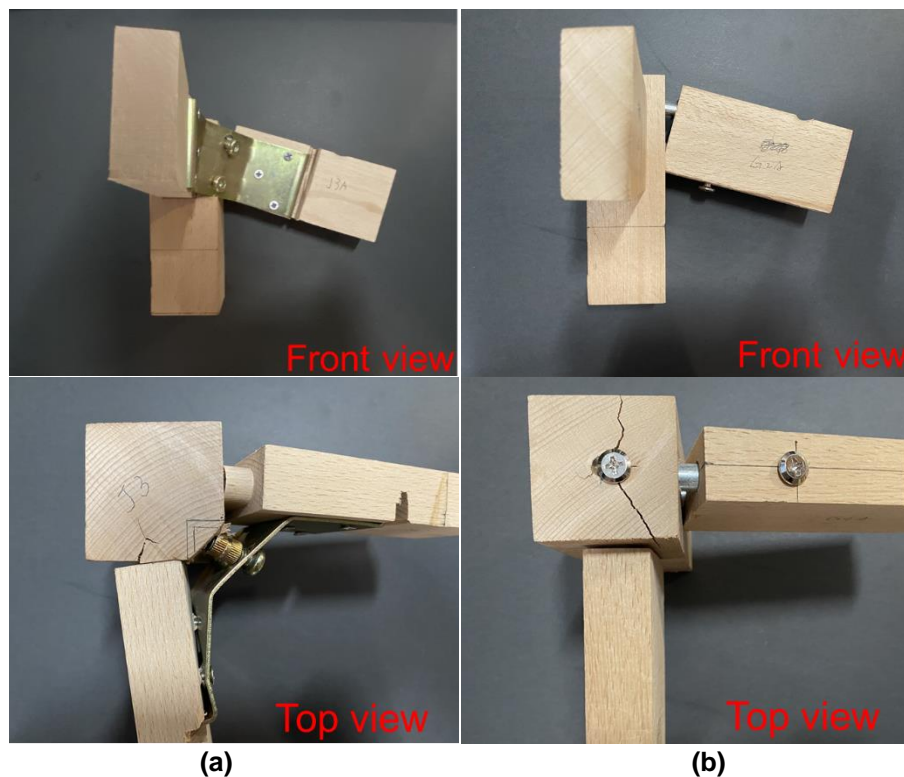


**Fig. 10.** The failure mode of the two experimental joints: commonly used detachable joint (a); and novel joint I (b)

In the case of the control joint, plastic deformation initially occurred at the rail member where the loading head applied deflection failures. The failure occurred at the tenon and mortise, which indicated that the tenon was gradually pulled out from the mortise. Therefore, the metal plug plastically distorted with the screws, and the embedded nuts were completely pulled out. Finally, the metal plug slots were widened with the embedded nuts

to bring out some wood fibers (Fig. 10a). Apparently, fractures also appeared at the edge of the other post number without applying loads, owing to the withdrawal strength of the screws, *i.e.*, the failure of one side of the post will directly affect the stability of the other rail component. In novel joint I, the failure first appeared at the prefabricated hole of the bolt and gradually extended to the whole section of post members, as the displacement increased (Fig. 10b). However, all tested specimens kept holding loads for a while after the fracture occurred and retained higher mechanical strength at the end of testing compared with the control joints. All the prefabricated holes through which the bolts and nuts were passed were plastically expanded and the transverse in-line double-hole nuts were severely bent under the compressive loads, which was because the stiffness of the metal connector far exceeded the wood material. In general, the typical failure modes were consistent with the diagram of stress distribution output from the FEM software, which verifies the efficiency of the simulation method.

All aforementioned discussion based on the numerical and experimental results implied that the novel bolt connection used in the corner joints proposed in this study was more convenient for assembly and processing. Furthermore, they had better bending strength performance and stability. However, only the stress distribution and magnitude relationship between the control joint and the novel joint I were compared and analyzed *via* FEM. Further study will pay additional attention to the methods of establishing the finite element model, *e.g.*, the fitting relationship and the contact characteristics between furniture elements, in order to accurately predict the mechanical strength performance of joints used in wood furniture frames.

## CONCLUSIONS

1. Three novel detachable joints used to connect a three-dimensional corner joint composed of two rails and one post leg were proposed.
2. The numerical analysis showed that novel joint I had good mechanical performance when subjected to bending load.
3. The experimental tests showed that the bending load resistance of the optimal joint (4386.57 N) was much higher than the commonly used joint (1921.25 N), as well as being more easily disassembled and had a lower coefficient of variance in terms of mechanical performance.

## ACKNOWLEDGMENTS

This research was partially supported by the Postgraduate Research & Practice Innovation Program of Jiangsu Province (KYCX\_0905), and partially supported by the Scientific Research Foundation of Nanjing Forestry University (GXL2019074) and partially supported by the Project from International Cooperation Joint Laboratory for Production, Education, Research and Application of Ecological Health Care on Home Furnishing. In addition, this study was also funded by the National First-class Disciplines (PNFD), and the Priority Academic Program Development of Jiangsu Higher Education Institutions (PAPD).

## REFERENCES CITED

- ASTM D2395 (2017). "Standard test methods for density and specific gravity (relative density) of wood and wood-based materials," ASTM International, West Conshohocken, PA.
- ASTM D4442 (2020). "Standard test methods for direct moisture content measurement of wood and wood-based materials," ASTM International, West Conshohocken, PA.
- Chen, Y., and Wu, Z. (2018). "Study on structure optimization design of modified wood furniture tenon structure based on the finite element analysis of ANSYS," *Journal of Intelligent & Fuzzy Systems* 34(2), 913-922. DOI: 10.3233/JIFS-169385
- Chen, Y., and Xu, W. (2017). "Mechanical properties of poplar table legs reinforced with improved structure," *China Wood Industry* 31(3), 44-48. DOI: 10.19455/j.mcgy.20170310
- Eckelman, C. A. (1978). *Strength Design of Furniture*, Tim Tech, Inc., West Lafayette, IN.
- Eckelman, C. A. (2003). *Textbook of Product and Strength Design of Furniture*, Purdue University, West Lafayette, IN.
- Eckelman, C. A., and Haviarova, E. (2006). "Performance tests of school chairs constructed with round mortise and tenon joints," *Forest Products Journal* 56(3), 51-57.
- Erdil, Y. Z., Kasal, A., and Eckelman, C. A. (2005). "Bending moment capacity of rectangular mortise and tenon furniture joints," *Forest Products Journal* 55(12), 209-213.
- Fu, W.-L., Guan, H.-Y., and Kei, S. (2021b). "Effects of moisture content and grain direction on the elastic properties of beech wood based on experiment and finite element method," *Forests* 12(5), 1-17. DOI: 10.3390/f12050610
- Fu, W.-L., Guan, H.-Y., and Zhang, X.-Y. (2021a). "Verification and further study on method of measuring contact force between mortise and tenon joint," *BioResources* 16(1), 263-276. DOI: 10.15376/biores.16.1.263-276
- Hajdarević, S., and Martinović, S. (2014). "Effect of tenon length on flexibility of mortise and tenon joint," *Procedia Engineering* 69, 678-685. DOI: 10.1016/j.proeng.2014.03.042
- Hu, W., and Liu, N. (2020). "Comparisons of finite element models used to predict bending strength of mortise-and-tenon joints," *BioResources* 15(3), 5801-5811. DOI: 10.15376/biores.15.3.5801-5811
- Hu, W., Chen, B., and Zhang, T. (2021). "Experimental and numerical studies on mechanical behaviors of beech wood under compressive and tensile states," *Wood Research* 66(1), 27-37. DOI: 10.37763/wr.1336-4561/66.1.2738
- Kasal, A., Smardzewski, J., Kuşkun, T., and Erdil, Y. Z. (2016). "Numerical analyses of various sizes of mortise and tenon furniture joints," *BioResources* 11(3), 6836-6853. DOI: 10.15376/biores.11.3.6836-6853
- Kaygin, B., Yorur, H., and Uysal, B. (2016). "Simulating strength behaviors of corner joints of wood constructions by using finite element method," *Drvna Industrija* 67(2), 133-140. DOI: 10.5552/drind.2016.1503
- Krzyżaniak, Ł., and Smardzewski, J. (2021). "Impact damage response of L-type corner joints connected with new innovative furniture fasteners in wood-based composites panels," *Composite Structures* 255, 1-11. DOI: 10.1016/j.compstruct.2020.113008

- Krzyżaniak, Ł., Smardzewski, J., and Prekrat, S. (2020). “Numerical modelling of stiffness of RTA furniture with new externally invisible and dismountable joints,” *Drvna Industrija* 71(2), 207-212. DOI: 10.5552/drvind.2020.1953
- Li, W., Gao, Y., Meng, X., Hu, Q., and Qiu Y. (2020). “Study on compressive performance of angel steel-glued laminated timber L-shaped composite column,” *Journal of Forestry Engineering* 5(1), 53-60. DOI: 10.13360/j.issn.2096-1359.201903025
- Likos, E., Haviarova, E., Eckelman, C. A., Erdil, Y. Z., and Ozcifci, A. (2012). “Effect of tenon geometry, grain orientation, and shoulder on bending moment capacity and moment rotation characteristics of mortise and tenon joints,” *Wood and Fiber Science* 44(4), 462-469.
- Liu, X. Y., Lv, M. Q., Liu, M., and Lv, J. F. (2019). “Repeated humidity cycling’s effect on physical properties of three kinds of wood-based panels,” *BioResources* 14(4), 9444-9453. DOI: 10.15376/biores.14.4.9444-9453
- Podskarbi, M., Smardzewski, J., Moliński, K., and Molińska-Glura, M. (2017). “Design methodology of new furniture joints,” *Drvna Industrija* 67(4), 371-380. DOI: 10.5552/drind.2016.1622
- Ratnasingam, J., and Ioras, F. (2013). “Effect of adhesive type and glue-line thickness on the fatigue strength of mortise and tenon furniture joints,” *European Journal of Wood and Wood Products* 71(6), 819-821. DOI: 10.1007/s00107-013-0724-1
- Uysal, M., Haviarova, E., and Eckelman, C. A. (2015). “A comparison of the cyclic durability, ease of disassembly, repair, and reuse of parts of wooden chair frames,” *Materials & Design* 87, 75-81. DOI: 10.1016/j.matdes.2015.08.009
- Wu, G., Sun, J., Huang, C., Ren, H., and Zhao, R. (2020). “Research progress on mechanical properties of tenon-and-mortise joints in traditional Chinese wood structures,” *Journal of Forestry Engineering* 5(4), 29-37. DOI: 10.13360/j.issn.2096-1359.201908030
- Wu, Y., Zhou, J.-C, Yang, F., Wang, Y.-J, Wang, J., and Zhang, J.-L. (2021). “A strong multi-layered transparent wood with natural wood color and texture,” *Journal of Materials Science* 56, 8000-8013. DOI: 10.1007/s10853-021-05833-1
- Xi, X., Yang, Y., and Zhang, Z. (2020). “Pull-out force and finite element analysis of T-type components of *Vitex negundo* L. scrimber with different node forms,” *Journal of Forestry Engineering* 5(1), 182-187. DOI: 10.13360/j.issn.2096-1359.201804018
- Yan, X.-X., Wang, L., and Qian, X.-Y. (2020). “Influence of the PVC of glass fiber powder on the properties of a thermochromic waterborne coating for Chinese Fir boards,” *Coatings* 10, 588. DOI: 10.3390/coatings10060588
- Yang, L., and Liu, H.-H. (2020). “Effect of a combination of moderate-temperature heat treatment and subsequent wax impregnation on wood hygroscopicity, dimensional stability, and mechanical properties,” *Forests* 11(9), 1-9. DOI: 10.3390/f11090920
- Yin, Q., and Liu, H.-H. (2021). “Drying stress and strain of wood: A review,” *Applied Sciences-Basel* 11(11), 1-19. DOI: 10.3390/app11115023
- Yu, M., Sun, D., Zou, W., Wang, Z., Jiang, X., Yao, L., and Kong, J. (2021). “Mechanical analysis of new Chinese style wood chairs using ANSYS,” *Journal of Forestry Engineering* 6(3), 178-184. DOI: 10.13360/j.issn.2096-1359.202006021
- Zhao, Z., Wu, D., Huang, C., Zhang, M., Umemura, K., and Yong, Q. (2020). “Utilization of enzymatic hydrolysate from corn stover as a precursor to synthesize an eco-friendly adhesive for plywood II: Investigation of appropriate manufacturing

- conditions, curing behavior, and adhesion mechanism,” *Journal of Wood Science* 66(1), 1-10. DOI: 10.1186/s10086-020-01933-9
- Zhou, C., Yu, M., and Zhou, T. (2018). “Experimental study on three-dimensional shape mapping of complex furniture,” *EURASIP Journal on Image and Video Processing* 2018, 1-9. DOI: 10.1186/s13640-018-0311-9
- Zhou, Y., Xue, Z., Huang, Q., Yao, B., and Wang, X. (2020). “Physical and mechanical properties of *Aucoumea klaineana* wood after vacuum heat treatment for furniture components,” *Journal of Forestry Engineering* 5(4), 73-78. DOI: 10.13360/j.issn.2096-1359.201907014
- Zor, M., and Kartal, M. E. (2020). “Finite element modeling of fiber reinforced polymer-based wood composites used in furniture construction considering semi-rigid connections,” *Drvna Industrija* 71(4), 339-345. DOI: 10.5552/drvind.2020.1916

Article submitted: December 18, 2021; Peer review completed: January 29, 2022;  
Revised version received: February 15, 2022; Accepted: February 16, 2022; Published:  
February 16, 2022.

DOI: 10.15376/biores.17.2.2143-2156